Crustal Deformation in the San Francisco Bay Area

The views and conclusions contained in this document are those of the authors and should not be interpreted as necessarily representing the official policies, either expressed or implied, of the U.S. Government.

USGS Award No.: 1434-HQ-97-GR-03122

Paul Segall and Mark H. Murray
Stanford University
Geophysics Department
Stanford CA 94305-2215

Tel: 650-725-7241 and 650-723-9594 (respectively)
Fax: 650-725-7344
URL: http://pangea.stanford.edu/deform

Program Element: II, III

Key Words: GPS campaign, GPS continuous, Fault Dynamics, Fault Stress Interactions

Non-technical Summary

This project focuses on integration and modeling of geodetic measurements in the San Francisco Bay area. We combine previously collected Geodolite (precise laser distance measurements), Global Positioning System (GPS), and Very Long Baseline Interferometry (VLBI) measurements to determine the deformation field in the Bay area and to study how seismic stain accumulates on the principal faults. We also re-examine triangulation measurements made after the 1906 earthquake to study post-seismic relaxation and stress transfer, and perform time-dependent inversions and finite element calculations to study the fault geometry in the lower crust and stressing-rates on Bay area faults.

Investigations Undertaken

The primary goal of this project is to synthesize the deformation field in northern California, with emphasis on the populated San Francisco Bay region. We are combining Global Positioning System (GPS), Geodolite trilateration (EDM) and very-long-baseline interferometry (VLBI) observations, and positions and velocities derived from these observations, primarily from U. S. Geological Survey (USGS) and Stanford University field campaigns and the Bay Area Regional

Deformation (BARD) permanent GPS network in northern California. Combining these data will enable us to clarify the rates of interseismic strain accumulation on the principal Bay area faults: the San Andreas, Hayward, and Calaveras faults, and their extensions north of the San Francisco Bay. We are also analyzing deformation following major northern California earthquakes, including the 1906 San Francisco and 1989 Loma Prieta earthquakes, to better understand post-seismic relaxation and stress transfer. Finally, time-dependent inversions and finite-element calculations will improve our understanding of the structure and rheology of the sub-seismogenic crust in the San Francisco Bay area.

Results

1. Strain accumulation rates in the San Francisco Bay area, 1972-1989

In Savage et al. (1998), we present strain accumulation rates in the San Francisco Bay area constructed from trilateration observations extending from about 1972 until the Loma Prieta earthquake in late 1989. The observations were corrected to remove offsets imposed by shallow fault creep and by four M~6 earthquakes that occurred in the Bay area during that time interval. The Bay area was divided into 32 contiguous polygons (Fig. 1), and the uniform (in both space and time) strain rates that best explain the changes in the corrected distances within each polygon were calculated. In a coordinate system with the 1 axis directed N58°E and the 2 axis N32°W (perpendicular and parallel to the local tangent to the small circle drawn about the Pacific--Sierra Nevada pole of rotation) the average of these 32 strain rates (each weighted by the area of the polygon) are ε_{11} = 9.2±7.4, ε_{12} = -160.7±4.6, and ε_{22} = 8.2±6.2 nanostrain/yr, where extension is reckoned positive and quoted uncertainties are standard deviations. As expected from the Pacific-Sierra Nevada relative plate motion, the overall strain rate is predominantly right-lateral shear across a vertical plane striking N32°W (Fig. 1). The net increase in the 12,225 km² area of the trilateration network is only 212±110 m²/yr, which arises from almost equal extensions in the N32°W and N58°E directions. Within the networks the strain rates vary from polygon to polygon. The N58°E extension rate is positive in 22 of the 32 polygons (Fig. 2), a proportion that is significantly larger than would be expected by chance if the N58°E extension rate were zero or negative. Significant areal dilatation rates are observed in almost 1/3 of the individual polygons and the N32°W extension rates tend to be negative to the west of the Hayward-Rodgers Creek fault trend and positive east of it

(Fig. 3). The pre-1989 strain accumulation across the eventual site of the Loma Prieta rupture involves fault normal contraction as well as right-lateral shear, consistent with the rupture mechanism.

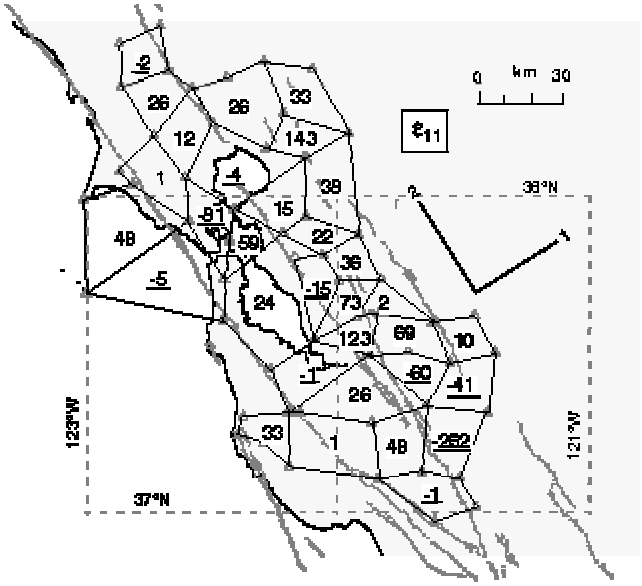

Figure 1. The average strain rate (right-lateral shear across a vertical plane striking N32°W) in the San Francisco Bay area within each of the 32 polygonal regions, in nanostrain/yr (boldface type indicates rates that differ from 0 at the 95% confidence level).

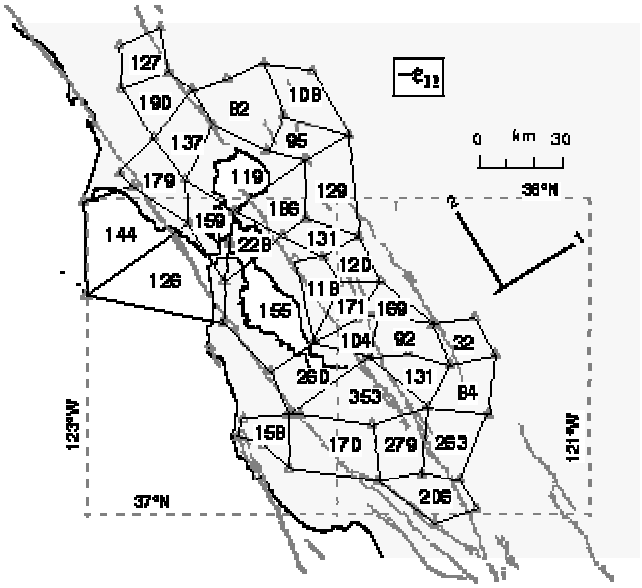

Figure 2. The average strain rate (fault-normal extension) in the San Francisco Bay area (conventions as in Figure e12). The predominant

positive (extension) signal in the entire network suggests that its source is not the strike-slip mechanisms of the dominant faults.

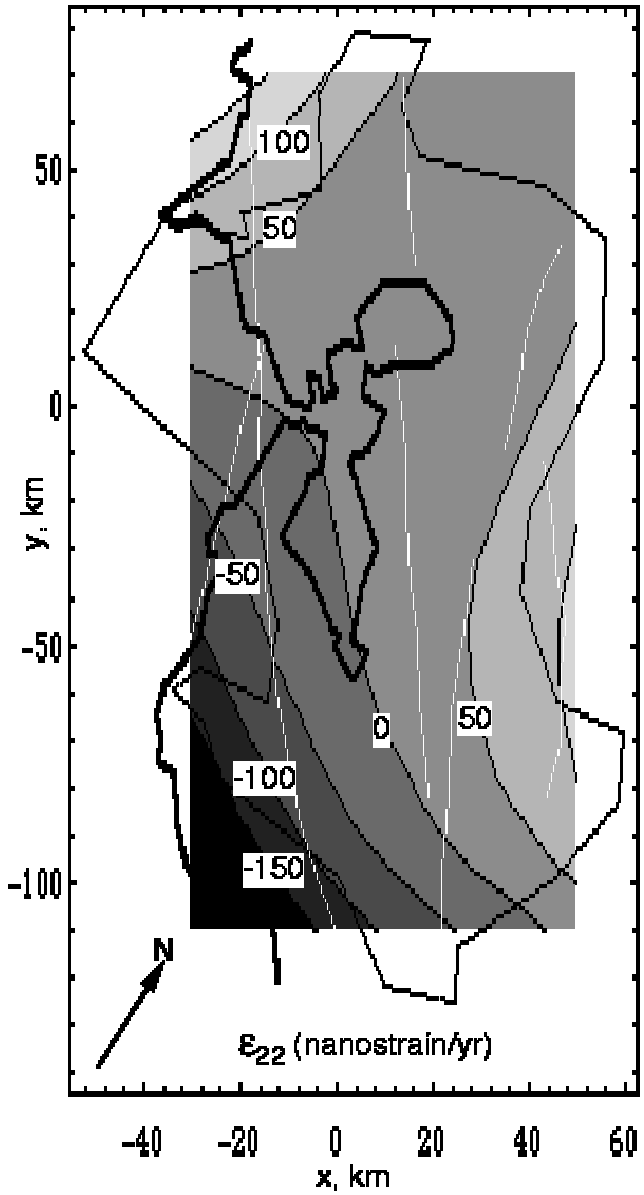

Figure 3. The average strain rate (fault-parallel extension) contoured using a third-degree polynomial approximation. Faults shown by sinuous white lines. The east Bay tends to be more positive and the southwest Bay tends to be more negative. This may be due to the systematic differences in orientation between the faults located in each region and the average N32°W trend (the east Bay faults tend to be oriented more easterly, and west Bay faults tend to be more westerly).

2. Kinematics of the Pacific-North America plate boundary zone, northern California

In Freymueller et al. (1999), we develop methods for assessing uncertainties of fault slip and geometry models and apply these methods to a crustal deformation study in northern California, principally along the San Andreas fault system in the northern Coast Ranges. We intend to apply similar methods to the three-dimension fault models we are developing for the San Francisco Bay area as part of this project. In the northern California study we measured motions of 54 sites in an east-west transect across California at 38-40°N by Global Positioning System (GPS) observations over a four year span to study the plate boundary zone (Fig. 4). GPS velocities from this network place tight constraints on the total slip rate on the San Andreas fault system, which we estimate to be 40±1 mm/yr. Slip rates on the individual faults are determined less precisely due to the high correlations between estimated slip rates and locking depths, and between slip rates on adjacent faults (Fig. 5). Our best fitting model fits the fault-parallel velocities with a normalized rms of 1.0185, and the following estimated fault slip rates (all in mm/yr, with 68.6% confidence intervals): San Andreas $17.4^{+2.5}_{-3.1}$, Ma'acama $13.9^{+4.1}_{-2.8}$, Bartlett Springs $8.2^{+2.1}_{-1.9}$ (Fig. 6). The data are fit best by models in which the San Andreas fault is locked to $14.9^{+12.5}_{-7.1}$ km, the Ma'acama fault locked to $13.4^{+7.4}_{-4.8}$ km except for shallow creep in the upper 5 km, and the Bartlett Springs fault may be creeping at all depths. Our estimated slip rate on the San Andreas fault is lower than all geologic estimates, although the 95% confidence interval overlaps the range of geologic estimates. Our estimate of the Ma'acama fault slip rate is greater than slip rate estimates for the Hayward or Rodgers Creek faults, its continuation to the south. The Ma'acama fault most likely poses a significant seismic hazard, as it has a high slip rate and a slip deficit large enough to generate a magnitude 7 earthquake today since there have been no significant earthquakes on the fault in the historical record. The shallow creep observed on the Ma'acama fault relieves only a fraction of the tectonic stress. We find little or no geodetic evidence for contraction across the Coast Ranges, except possibly at western edge of Great Valley where 1-3 mm/yr of shortening is permitted by the data.

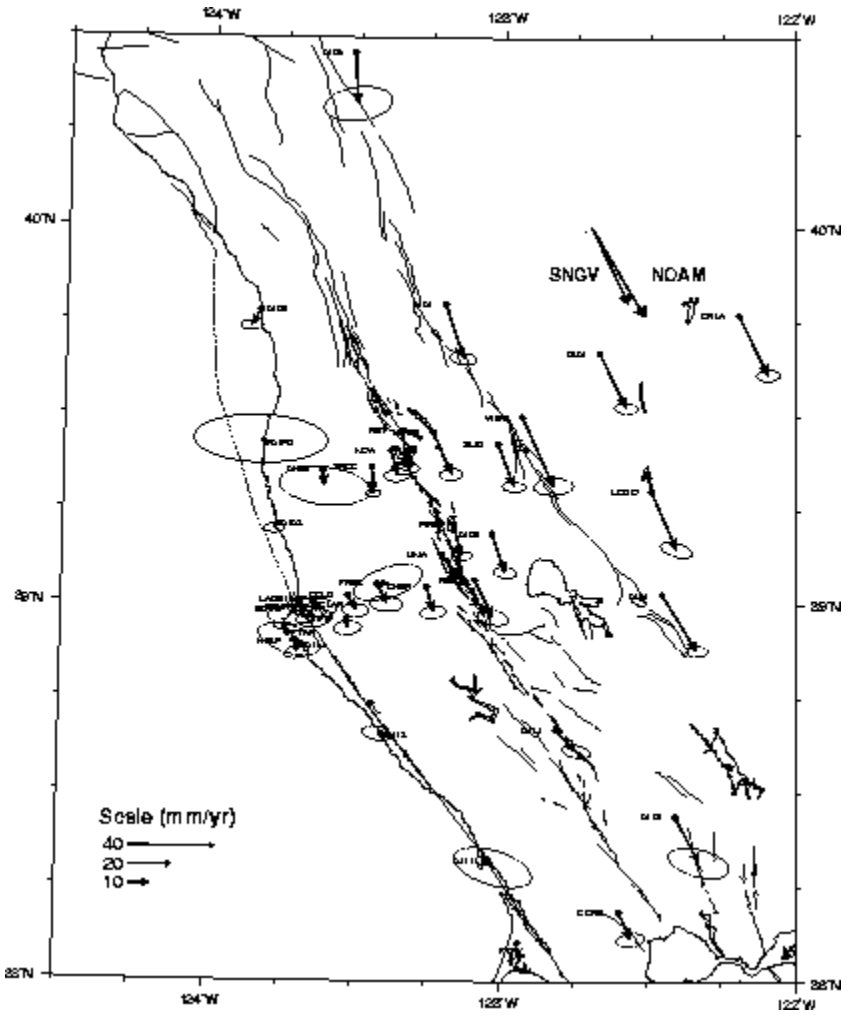

Figure 4. Velocities of GPS sites in the Coast Ranges and western Great Valley, relative to Point Reyes NCMN on the Point Reyes peninsula (38°N, 123°W) with 95% confidence regions. Virtually all velocities are parallel to the San Andreas fault system (sinuous NW-trending lines, principally comprised from west to east of the San Andreas, Ma'acama, and Bartlett Springs faults). The NOAM and SNGV arrows show predicted NUVEL-1A North America and Sierra Nevada--Great Valley motions (Don Argus, personal communication, 1998).

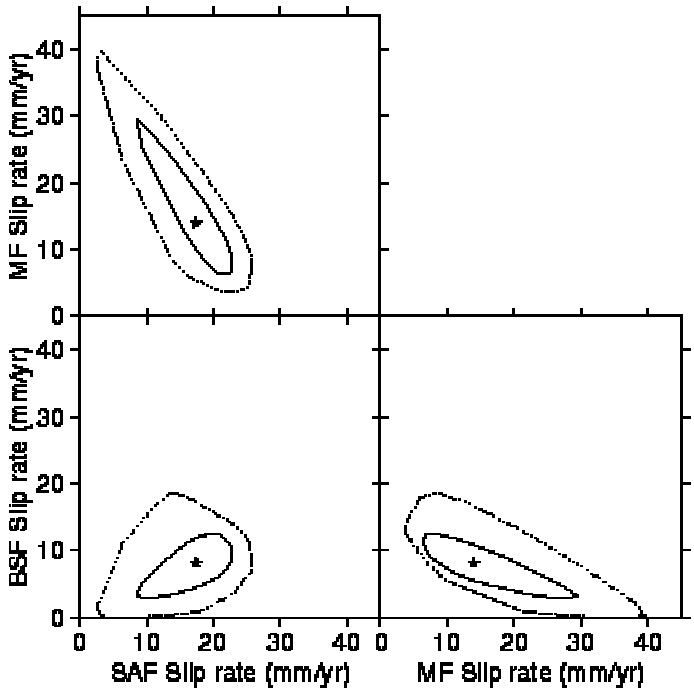

Figure 5. Optimal model and confidence regions for slip rates, showing correlations between the San Andreas (SAF), Ma'acama (MF), and Bartlett Springs (BSF) faults. The star indicates the optimal model determined by random cost optimization methods. Contours are 50% (solid) and 95% (dashed) confidence regions determined by bootstrapping (resampling with replacement) methods. Note the strong correlations between slip rates on adjacent faults, SAF and MF, and MF and BSF.

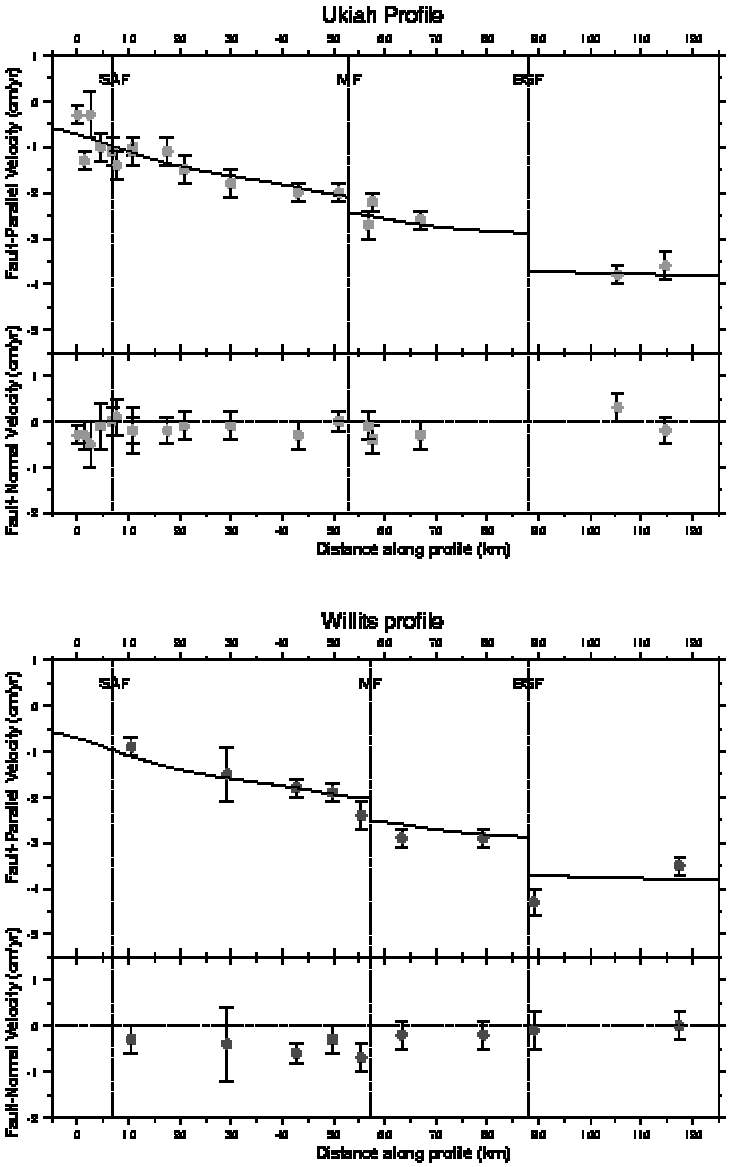

Figure 6. Ukiah (top) and Willits (bottom) profiles, showing fault-parallel and fault-normal velocities along with predictions of the optimal model. Fault-normal velocities were not modeled but are shown for reference. While total fault-parallel slip is 40±1 mm/yr, only 3±2 mm/yr of fault-normal shortening is observed between the Great Valley and Pacific Coast.

3. Crustal deformation in the northern California from VLBI, GPS, and Geodolite Data

We are in the process of combining measurements from the permanent GPS network in northern California with older VLBI and spatially dense Geodolite EDM measurements, and campaign GPS

measurements currently being collected by the USGS, Stanford University, and UC Berkeley. The combined velocity map will provide significantly improved constraints on three-dimensional locking depth and deep-slip models of strain accumulation, which will be used for seismic hazard assessment along the San Andreas fault system.

Murray et al. (1998b) and Prescott et al. (1998) presented estimated velocities for the Bay Area Regional Deformation (BARD) network of ~35 permanent GPS sites in northern California. The velocities, averaged over the 1993.8-1998.8 interval, are shown in Figure 7 relative to stable North America as defined by the five IGS fiducial stations. The Farallon Island site off the coast of San Francisco is moving at nearly the rate predicted by the NUVEL-1A Pacific-North America Euler pole. Most of the Sierra Nevada and Great Valley sites, show little relative motion, indicating that the northern Sierra Nevada-Great Valley is tectonically stable. The motion of these sites relative to North America is consistent with spreading in the Basin and Range Province. The sites near Long Valley caldera show anomalously high radial motions away from the center of the caldera, consistent with inflation of magmatic sources at depth. Deformation along the coast is dominated by the active San Andreas fault system, which accommodates about 35 mm/yr of right-lateral shear (Fig. 8).

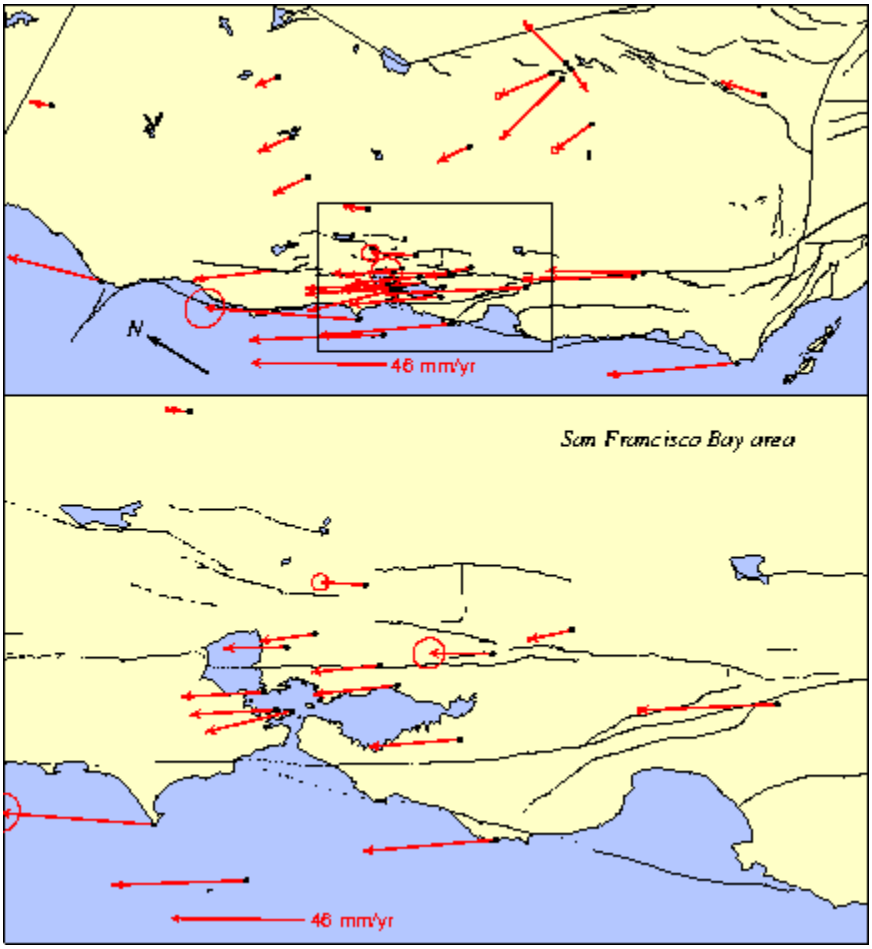

Figure 7. Average velocities of BARD stations in northern California (top) and in the San Francisco Bay area (bottom) with 95% confidence regions (Murray et al., 1998b). The oblique Mercator projection is about the NUVEL-1A Pacific-North America Euler pole so that expected relative plate motion is parallel to the horizontal. The NUVEL-1A predicted 46 mm/yr Pacific-North America relative motion is shown for scale. Velocities are relative to stable North America.

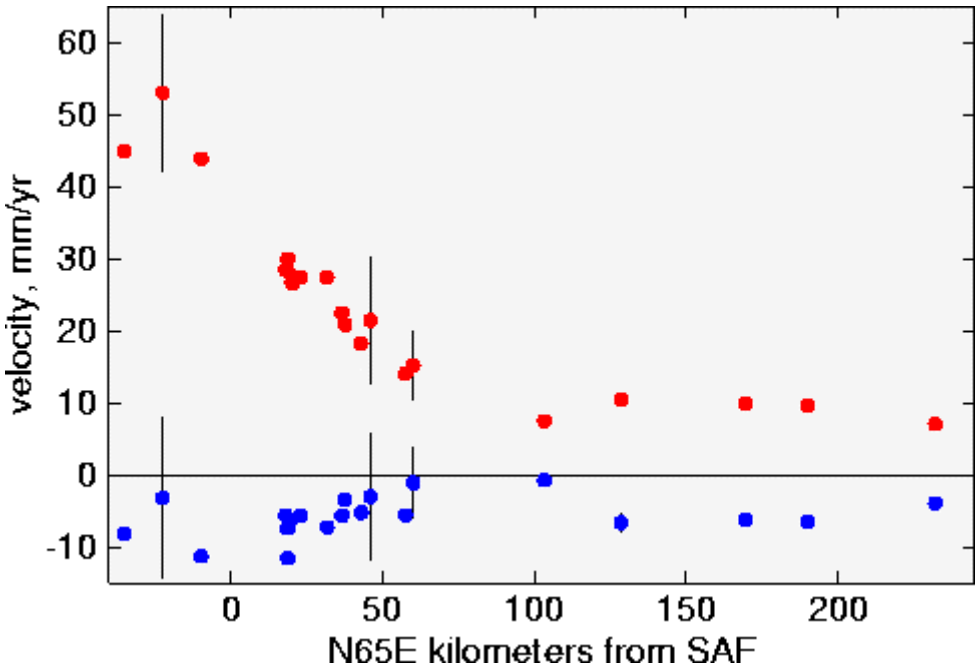

Figure 8. Velocities of the BARD sites parallel (red) and perpendicular (blue) to the average N35°W strike of the SAF system. The majority (~35 mm/yr) of the predicted right-lateral plate boundary deformation is accommodated across a 100-km zone straddling the San Andreas fault system. The motion of the westernmost site on the Farallon Islands is in agreement with the NUVEL-1A predicted rate for the Pacific plate, suggesting that little additional deformation is required offshore. The coastal stations have a consistent clockwise rotation, between 5-10 mm/yr. We are currently investigating reference frame definition problems as a possible explanation for these motions.

Murray et al. (1998a) presented estimated average velocites for sites in the San Francisco Bay area from campaign GPS observations, primarily collected over the 1993-1998 interval by the U.S. Geological Survey. Figure 9 shows the average velocites for the 5 roughly parallel profiles crossing the San Andreas fault system measured annually by the USGS. We are working with Will Prescott and Jerry Svarc (USGS), who analyzed the measurements and provided the 155 station coordinate and covariance solutions. We combined these solutions, which were estimated assuming weakly constrained a priori fiducial coordinates, to estimated the position and velocity of 113 stations. We then applied strong a posteriori constraints to define a North America-fixed reference frame as realized by the 10 IGS fiducial stations they had included in their solutions. This methodology ensures the velocities are estimated in a self-consistent reference frame.

The resulting interseismic deformation field is consistent with the permanent GPS network results (Fig. 7), but allows a more comprehensive assessment of the distribution of deformation both across and along the San Andreas fault system. We are in the process of combining these results with the previously discussed Geodolite and BARD permanent GPS results, with VLBI observations provided by the Goddard Space Flight Center, and with other campaign GPS observations primarily collected in the south Bay by Roland Burgmann (UC Berkeley). We have also begun to develop three-dimensional fault interseismic-slip models, following the geometry and methodology described in Williams (1995). Results from these and similar models will be used in the USGS-led Working Group 99 effort to reevaluate earthquake probabilities in the San Francisco Bay area.

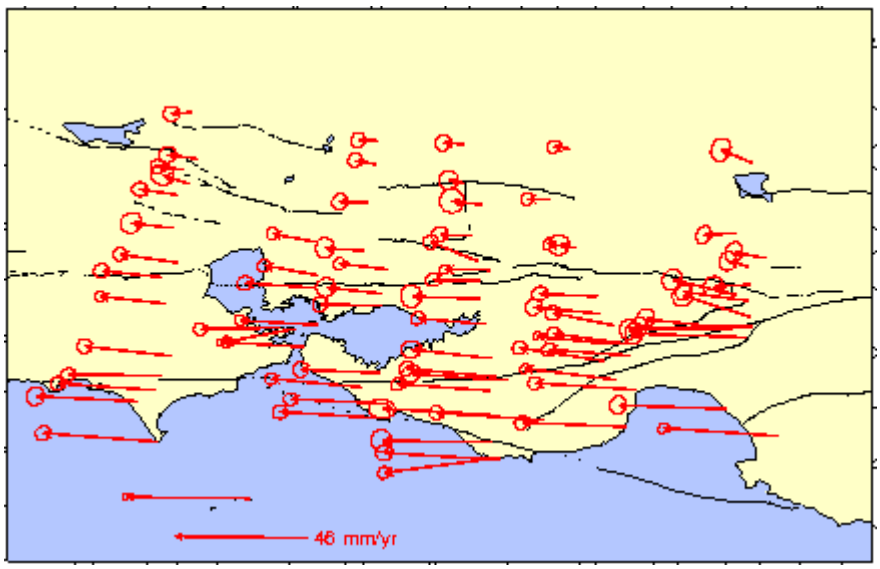

Figure 9. Velocities of campaign GPS sites in the San Francisco Bay area measured annually by the USGS during 1993-1998, with 95% confidence regions. The projection is the same as in Figure 7. The velocities are relative to stable North America as defined by 10 IGS fiducial stations.

4. Post-seismic deformation of the 1906 San Francisco earthquake in northern California

Thatcher's work (1975a, 1975b, and 1983) represents the primary source of information on the nature of postseismic deformation after great earthquakes within the San Andreas fault system. We have, therefore, re-evaluated the available triangulation data from northern California following the 1906 San Francisco earthquake using the improved methods of Yu and Segall (1996). These methods make use

of all the available data. Prior analysis have been limited to the use of only repeated angles. As a result, we have both increased the number and extended the spatial resolution of existing constraints on the nature of postseismic deformation following great events on the San Andreas fault. We have calculated uniform shear strain rates and made velocity estimates for two networks, one at Pt. Arena, California and the second extending from Pt. Reyes Head, California to Petaluma, California. With the inclusion of more recent GPS results, we have also been able to infer relaxation times for long-term, postseismic deformation following the 1906 earthquake at both localities. Finally, for both networks, we have been able to investigate spatial and temporal variations in the velocity field by exploring probable models of deformation at depth using a grid search approach to identify optimal accelerated deep afterslip and detachment models. We also investigated data from the Northern California Primary Network which includes the Farallon Islands. Unfortunately, the baseline lengths within this network were too large to permit reasonable velocity estimates.

Specifically, using triangulation data obtained from the National Geodetic Survey, two inversions were completed at Pt. Arena. The first used data from three surveys, 1906-07, 1925, and 1929-30. The second used data from two surveys, 1929-30 and 1973-75. Two inversions of triangulation data were also completed using data from the Petaluma Arc. The first used data from 1929-30 and 1938-39, while the second used data from 1938-39 and 1960-61. Each of the inversions assumed constant velocities throughout the time interval under consideration. GPS results from 1991 to 1995 at Pt. Arena (Freymueller et al., in press) and from 1991 to 1993 at the location of the Petaluma Arc (Williams, 1995) were then compared to the triangulation results.

Based solely on uniform shear strain rate data from Pt. Arena, we find an exponential relaxation time for long-term postseismic deformation following the 1906 earthquake of 29±15 yrs (Fig. 10). Preliminary calculations using strain rate data from a subnet of the Petaluma Arc immediately adjacent to the fault are similar. Both these results agree with the prior estimates of approximately 30 yrs using strain rate data from the entire San Andreas fault (Thatcher, 1983). Because of a lack of spatial resolution, particularly at Pt. Arena, individual inversions for the optimal models are not well constrained. When taken in total, though, the inversion results do permit some conclusions. At both Pt. Arena and Petaluma, the rate of deformation must change with time. At Pt. Arena, the model coordinate station velocities, which show no

obvious asymmetry, can be satisfactorily fit with accelerated afterslip at depth along the San Andreas fault plane. Further, inversion results indicate that slip velocity decreases by approximately 50% between 1906-30 and 1929-75 and that the top of the zone of accelerated afterslip located at approximately 9-10 km depth. In contrast, data from the Petaluma Arc clearly show asymmetric deformation, especially between 1929 and 1939. Accelerated deep afterslip and horizontal detachment models have trouble explaining the observed deformation field, particularly to the west of the San Andreas fault. To the east, both of these simple models have trouble predicting the breadth and linearity of the velocity profiles. A more complex mechanism is therefore required to explain the results from the Petaluma Arc.

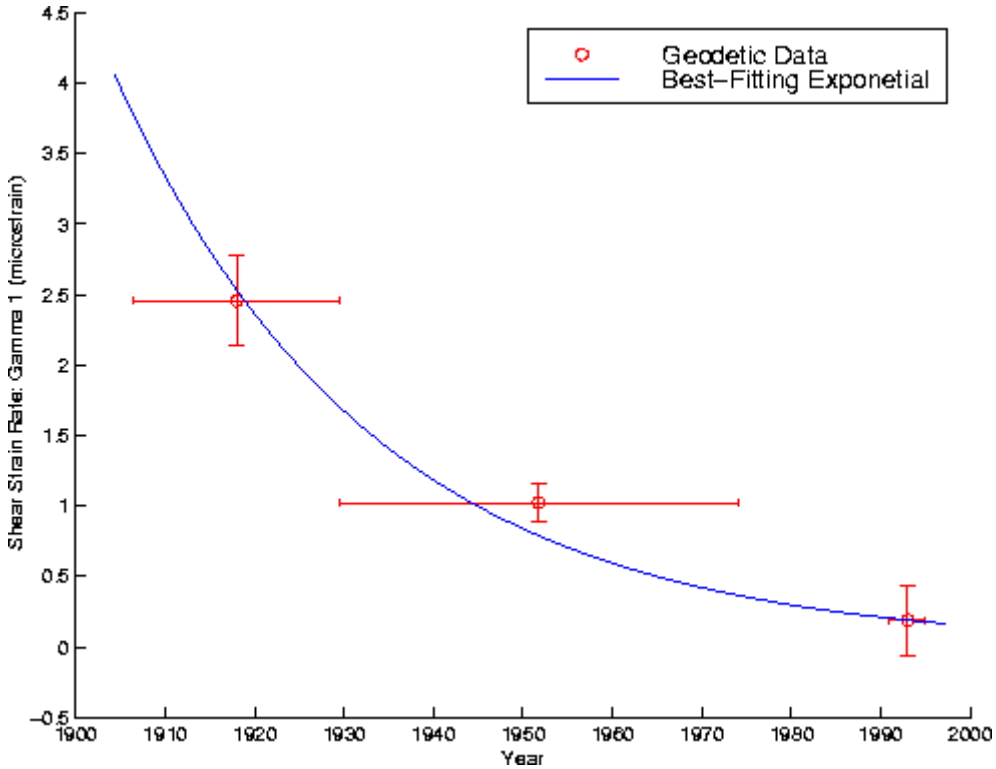

Figure 10. Evolution of uniform shear strain rate with time since the 1906 San Francisco earthquake at Pt. Arena, California. Vertical error bars give 1 sigma uncertainties. Horizontal error bars give the time between the first and last surveys included in the inversion.

Reports Published

Freymueller, J. T., M. H. Murray, P. Segall, and D. Castillo, Kinematics of the Pacific-North America plate boundary zone, northern California, J. Geophys. Res., in press, 1999.

Kenner, S. J., and P. Segall, Re-evaluation of postseismic deformation at Point Arena, California following the 1906 San Francisco earthquake (abstract), EOS Trans AGU, 79(45), Fall Meeting Suppl., F601, 1998.

Kenner, S. J., and P. Segall, Time-dependence of the stress shadowing effect and its relation to the structure of the lower crust, Geology, in press, 1999.

Murray, M. H., W. H. Prescott, R. Burgmann, J. T. Freymueller, P. Segall, J. Svarc, S. D. J. Williams, M. Lisowski, and B. Romanowicz, The deformation field of the Pacific-North America plate boundary zone in northern California from geodetic data, 1973-1989 (abstract), EOS Trans. AGU, 79(45), Fall Meeting Suppl., F192, 1998a.

Murray, M. H., R. Burgmann, W. H. Prescott, B. Romanowicz, S. Schwartz, P. Segall, and E. Silver, The Bay Area Regional Deformation (BARD) permanent GPS network in northern California (abstract), EOS Trans. AGU, 79(45), Fall Meeting Suppl., F206, 1998b.

Prescott, W. H., R. Baxter, R. Burgmann, M. Murray, B. Romanowicz, J. Savage, J. Svarc, and K. Wendt, Broad scale deformation across the Pacific-North America boundary in northern California (abstract), EOS Trans. AGU, 79(45), Fall Meeting Suppl., F192, 1998.

Savage, J. C., R. W. Simpson, and M. H. Murray, Strain accumulation rates in the San Francisco Bay area, 1972-1989, J. Geophys. Res., 103, 18,039-18,051, 1998.

Segall, P., and M. V. Matthews, Time dependent inversion of geodetic data, J. Geophys. Res., 102, 22,391-22,409, 1997.

Other References

Thatcher, W., Strain accumulation and release mechanism of the 1906 San Francisco earthquake, J. Geophys. Res., 80, 4862-4872, 1975a.

Thatcher, W., Strain accumulation on the northern San Andreas fault zone since 1906, J. Geophys. Res., 80, 4873-4880, 1975b.

Thatcher, W., Nonlinear strain buildup and the earthquake cycle on the San Andreas fault, J. Geophys. Res., 88, 5893-5902, 1983.

Williams, S. D. P., Current motion on faults of the San Andreas system in Central California inferred from recent GPS and terrestrial survey measurements, Ph.D. Dissertation, Department of Geological Sciences, University of Durham, 269 pp., 1995.

Yu, E. and P. Segall, Slip in the 1868 Hayward earthquake from the analysis of historical triangulation data, J. Geophys. Res., 101, 16,101-16,118, 1996.